

Ceramide glycosylation potentiates cellular multidrug resistance

YONG-YU LIU, TIE-YAN HAN, ARMANDO E. GIULIANO, AND MYLES C. CABOT¹

John Wayne Cancer Institute at Saint John's Health Center, Santa Monica, CA 90404, USA

ABSTRACT Ceramide glycosylation, through glucosylceramide synthase (GCS), allows cellular escape from ceramide-induced programmed cell death. This glycosylation event confers cancer cell resistance to cytotoxic anticancer agents [Liu, Y. Y., Han, T. Y., Giuliano, A. E., and M. C. Cabot. (1999) *J. Biol. Chem.* 274, 1140–1146]. We previously found that glucosylceramide, the glycosylated form of ceramide, accumulates in adriamycin-resistant breast carcinoma cells, in vinblastine-resistant epithelioid carcinoma cells, and in tumor specimens from patients showing poor response to chemotherapy. Here we show that multidrug resistance can be increased over baseline and then totally reversed in human breast cancer cells by GCS gene targeting. In adriamycin-resistant MCF-7-AdrR cells, transfection of GCS upgraded multidrug resistance, whereas transfection of GCS antisense markedly restored cellular sensitivity to anthracyclines, *Vinca* alkaloids, taxanes, and other anticancer drugs. Sensitivity to the various drugs by GCS antisense transfection increased 7- to 240-fold and was consistent with the resumption of ceramide-caspase-apoptotic signaling. GCS targeting had little influence on cellular sensitivity to either 5-FU or cisplatin, nor did it modify P-glycoprotein expression or rhodamine-123 efflux. GCS antisense transfection did enhance rhodamine-123 uptake compared with parent MCF-7-AdrR cells. This study reveals that GCS is a novel mechanism of multidrug resistance and positions GCS antisense as an innovative force to overcome multidrug resistance in cancer chemotherapy.—Liu, Y.-Y., Han, T.-Y., Giuliano, A. E., and Cabot, M. C. Ceramide glycosylation potentiates cellular multidrug resistance. *FASEB J.* 15, 719–730 (2001)

Key Words: glucosylceramide synthase • antisense • breast cancer • apoptosis • chemotherapy

CERAMIDE, A SECOND messenger in apoptotic signaling, plays a principal role in the nature of cellular response to anticancer therapies, participating in reactions to both chemotherapy and radiation (1, 2). Accumulation of glucosylceramide (GC) is a characteristic of some multidrug-resistant (MDR) cancer cells of breast, ovarian, colon, and epithelioid carcinomas (3–5). Drug resistance induced by *MDR1* transfection is accompanied by increased levels of GC (6). Further, preliminary clinical studies show that GC levels are elevated in tumor specimens from patients with breast cancer and

melanoma who demonstrated poor response to chemotherapy (7). The enzyme glucosylceramide synthase (GCS, ceramide glucosyltransferase, UDP-glucose:*N*-acylsphingosine D-glucosyltransferase, EC 2.4.1.80) transfers glucose from UDP-glucose to ceramide and produces GC. An increased capacity for ceramide glycosylation has been revealed in multidrug-resistant human breast carcinoma cells (8), and enhanced expression of GCS by gene targeting confers resistance to adriamycin and to tumor necrosis factor α in breast cancer cells (9, 10). In an opposing scenario, GCS antisense transfection can reverse adriamycin resistance in drug-resistant breast cancer cells (11). As ceramide glycosylation emerges as a novel mechanism of adriamycin resistance (3–5, 8, 9, 11), we hypothesized that decreasing the potential for ceramide glycosylation would be one avenue to overcome cellular resistance to several classes of anticancer drugs. To identify the role of GCS in multidrug resistance, and to explore a novel approach to reverse resistance, we introduced GCS sense and GCS antisense cDNA into adriamycin-resistant human breast carcinoma cells and assessed the influence of GCS on the nature of multidrug resistance, using classical antitumor agents belonging to the anthracycline, *Vinca* alkaloid, and taxane classes.

MATERIALS AND METHODS

Materials

[³H]UDP-glucose (40 Ci/mmol) was purchased from American Radiolabeled Chemicals (St. Louis, Mo.). [³H]Palmitic acid (56.5 Ci/mmol) was from DuPont/NEN (Boston, Mass.), and [*methy*-³H]thymidine (49.0 Ci/mmol) was from Amersham (Piscataway, N.J.). C₆-Ceramide (*N*-hexanoylsphingosine) was purchased from LC Laboratories (Woburn, Mass.). Sulfatides (ceramide galactoside 3-sulfate) were from Matreya (Pleasant Gap, Pa.), and phosphatidylcholine (1,2-dioleoyl-*sn*-glycero-3-phosphocholine) was from Avanti Polar Lipids (Alabaster, Ala.). Adriamycin (doxorubicin hydrochloride) and other chemicals were purchased from Sigma (St. Louis, Mo.). Silica Gel G thin-layer chromatography (TLC) plates were from Analtech (Newark, Del.). Fetal bovine serum (FBS) was purchased from HyClone (Logan, Utah). RPMI

¹ Correspondence: John Wayne Cancer Institute, 2200 Santa Monica Blvd., Santa Monica, CA 90404, USA. E-mail: Cabot@jwci.org

medium 1640 and DMEM medium (high glucose) were from Gibco BRL (Gaithersburg, Md.), and cultureware was from Corning Costar (Cambridge, Mass.). GCS antiserum was kindly provided by Drs. D. L. Marks and R. E. Pagano (Mayo Clinic and Foundation, Rochester, Minn.). Anti-Xpress tag antibody was from Invitrogen (Carlsbad, Calif.). C219, the monoclonal antibody against P-glycoprotein, was from Signet (Dedham, Mass.).

Cell lines and culture conditions

The human breast adenocarcinoma cell line, MCF-7-AdrR, which is resistant to adriamycin (12), was kindly provided by Dr. Kenneth Cowan (UNMC Eppley Cancer Center, Omaha, Neb.) and Dr. Merrill Goldsmith (National Cancer Institute, Bethesda, Md.). Cells were maintained in RPMI 1640 medium containing 10% (v/v) FBS, 100 U/ml penicillin, 100 µg/ml streptomycin, and 584 mg/liter L-glutamine. Cells were cultured in a humidified 5% CO₂ atmosphere tissue culture incubator and subcultured weekly using trypsin-EDTA (0.05%, 0.53 mM) solution. The stably transfected cells, MCF-7-AdrR/GCS and MCF-7-AdrR/asGCS, were cultured in RPMI 1640 medium containing 400 µg/ml G418 (geneticin) in addition to the above components.

Giemsa staining was performed as described (11). Cells were seeded in 60-mm dishes (10⁵ cells per dish) in 10% FBS RPMI 1640 medium and grown for 2 days at 37°C. After fixing, cells were stained with KaryoMAX Giemsa solution (Gibco BRL) and photomicrographed.

pcDNA 3.1/his-GCS and pcDNA 3.1/his A-asGCS expression vectors and transfection

pCG-2, a Bluescript II KS containing GlcT-1 (ref.13 terminology for GCS) in the *EcoRI* site, was kindly provided by Dr. Shinichi Ichikawa and Dr. Yoshio Hirabayashi (The Institute of Chemical and Physical Research, Saitama, Japan). The full-length cDNA of human GCS was subcloned into the *EcoRI* site in the pcDNA 3.1/His A with Xpress tag peptide (Invitrogen) in the upstream region. Xpress tag fuses at the NH₂ terminus of the cloned gene; therefore, GCS will be expressed as Xpress-GCS. The antisense- and sense-orientation of GCS cDNA was analyzed with Vector NTI 4.0 and doubly checked by restriction digestion. When MCF-7-AdrR cells reached 20% confluence, pcDNA 3.1-asGCS (GCS antisense) or pcDNA 3.1-GCS (10 µg/ml, 100-mm dish) were introduced by co-precipitation with calcium phosphate (Mammalian Transfection Kit; Stratagene, La Jolla, Calif.). The transfected cells were selected in RPMI 1640 medium containing 10% FBS and 400 µg/ml G418. Each G418-resistant clone, isolated using cloning cylinders, was propagated and later screened by GCS enzyme assay. pcDNA 3.1/his A plasmid was used in control transfections.

GCS assay

To determine the levels of GCS in the G418-resistant clones, a modified radioenzymatic assay was used (9, 14). Cells were homogenized by sonication in lysis buffer (50 mM Tris-HCl, pH 7.4, 1.0 µg/ml leupeptin, 10 µg/ml aprotinin, 25 µM PMSF). Microsomes were isolated by centrifugation (129,000 g, 60 min). The enzyme assay, containing 50 µg microsomal protein, in a final volume of 0.2 ml, was performed in a shaking water bath at 37°C for 60 min. The reaction contained a liposomal substrate composed of C₆-ceramide (1.0 mM), phosphatidylcholine (3.6 mM), and brain sulfatides (0.9 mM). Other reaction components included sodium phosphate buffer (0.1 M) pH 7.8, EDTA (2.0 mM), MgCl₂ (10

mM), dithiothreitol (1.0 mM), β-NAD (2.0 mM), and [³H]UDP-glucose (0.5 mM). Radiolabeled and unlabeled UDP-glucose were diluted to achieve the desired radiospecific activity (4,700 dpm/nmol). To terminate the reaction, tubes were placed on ice and 0.5 ml isopropanol and 0.4 ml Na₂SO₄ were added. After brief vortex mixing, 3 ml *t*-butyl methyl ether was added, and the tubes were mixed for 30 s. After centrifugation, 0.5 ml of the upper phase that contained GC was withdrawn and mixed with 4.5 ml EcoLume for analysis of radioactivity by liquid scintillation spectroscopy.

RNA analysis

Cellular mRNA was purified using a mRNA isolation kit (Boehringer Mannheim, Indianapolis, Ind.). Equal amounts of mRNA (5.0 ng) were used for reverse transcription polymerase chain reaction (RT-PCR), as described previously (11). Under upstream primer (5'-CCTTTCCTCTCCCCACCTTCTCT-3') and downstream primer conditions (5'-GGTTTCAGAAGAGACACCTGGG-3'), a 302-bp fragment in the 5'-terminal region of the GCS gene was produced using the ProSTAR HF single-tube RT-PCR system (High Fidelity, Stratagene) in a thermocycler (Mastercycler Gradient, Eppendorf). mRNA's were reverse transcribed using MMLV-reverse transcriptase at 42°C for 15 min. DNA was amplified with *TaqPlus* Precision DNA polymerase in a 40-cycle PCR reaction using the following conditions: denaturation at 95°C for 30 s, annealing at 60°C for 30 s, and elongation at 68°C for 120 s. RT-PCR products were analyzed by 1% agarose gel electrophoresis stained with ethidium bromide. β-actin was used as a control for consistent loading of gels.

Cytotoxicity assay

Assays were performed as described previously (9). Briefly, cells were seeded in 96-well plates (2×10³ cells per well) in 0.1 ml RPMI 1640 medium containing 10% FBS and cultured at 37°C for 24 h before addition of drug. Drugs were added in FBS-free medium (0.1 ml), and cells were cultured at 37°C for the indicated periods. Drug cytotoxicity was determined using the Promega 96 Aqueous cell proliferation assay kit (Promega, Madison, Wisc.). Absorbance at 490 nm was recorded using a Microplate Fluorescent Reader, model FL600 (Bio-Tek, Winooski, Vt.).

Colony formation in soft agar

The influence of GCS on cell growth in soft agar was analyzed by [³H]thymidine incorporation (15, 16). Cells (2×10⁴) were suspended in 0.5 ml RPMI 1640 medium (supplemented with 2 U/ml insulin and 10% FBS), containing 0.25% agarose III and the indicated concentrations of adriamycin. The mixture was added over a layer of 0.35% agar (0.5 ml) in RPMI 1640 medium in 24-well plates. After 72 h, 1.0 µCi [³H]thymidine was added to each well in 0.1 ml RPMI 1640 medium, and plates were maintained in the incubator an additional 48 h. Cells were harvested by heating (5 ml PBS, 100°C, 40 min) and centrifugation (1,000 g, 15 min), and lysed with KOH (0.075 M, 0.3 ml, 60 min). Cell lysates were mixed with 4 ml EcoLume for analysis of radioactivity by liquid scintillation spectroscopy.

Apoptotic cell death detection by ELISA and DNA fragmentation

The presence of mono- and oligonucleotides, a feature of cells undergoing apoptosis (17, 18), was evaluated by Cell

Death Detection ELISA, performed following kit instructions (Boehringer Mannheim). Briefly, cells were treated without or with the indicated concentration of adriamycin for 48 h, and 10^4 cells from each sample were lysed in 200 μ l lysis buffer. After centrifugation (1000 g, 10 min), a 20- μ l aliquot of lysate supernatant (10^3 cells per tube) was incubated with DNA-histone antibody and anti-DNA conjugated antibody for 2 h at 24°C and then incubated with substrate for 15 min. Absorbance was measured at 405 nm.

DNA fragmentation analysis was performed as described previously (10). Briefly, 0.5×10^6 cells were seeded in 10-cm dishes in medium containing 5% FBS. After attachment, cells were treated with 2 μ M adriamycin for 72 h. After harvest by trypsin-EDTA and centrifugation, cells were digested with lysis buffer (10 mM Tris-HCl, pH 8.0, 100 mM NaCl, 25 mM EDTA, 0.5% SDS, 0.3 mg/ml proteinase K). DNA was extracted with phenol/chloroform/isoamyl alcohol (25:24:1, v/v/v) and precipitated by incubating in one-half volume 7.5 M ammonium acetate plus two volumes 100% ethanol at -20°C overnight, followed by centrifugation (10,000 g, 20 min, 4°C). Contaminating RNA was digested in RNA-digestion buffer (10 mM Tris-HCl, 0.1 mM EDTA, 0.1% SDS, 100 U/ml RNase mixture). Re-extracted DNA (2–10 μ g) was analyzed by electrophoresis on a 2% agarose gel in TAE buffer (40 mM Tris acetate, 1 mM EDTA, pH 8.3) and was visualized with ethidium bromide under UV light.

Ceramide and glucosylceramide analysis

Analysis was performed as described previously (3, 9). Briefly, cells were seeded in 6-well plates (6×10^4 cells per well) in 10% FBS RPMI 1640 medium. After 24 h, cells were shifted to 5% FBS medium with or without agents and grown for the indicated times. Cellular lipids were radiolabeled by adding [3 H]palmitic acid (2.5 μ Ci/ml culture medium) for 24 h. After removal of medium, cells were rinsed twice with PBS (pH 7.4), and total lipids were extracted as described (9). The organic lower phase was withdrawn and evaporated under a stream of nitrogen. Lipids were resuspended in 100 μ l of chloroform/methanol (1:1, v/v), and aliquots were applied to TLC plates. Ceramide was resolved using a solvent system containing chloroform/acetic acid (90:10, v/v), and GC was resolved using a solvent system containing chloroform/methanol/ammonium hydroxide (70:20:4, v/v). Commercial lipid standards were co-chromatographed. After development, lipids were visualized with iodine vapor staining and identified by migration. The ceramide and GC area was scraped into 0.5 ml water. EcoLume counting fluid (4.5 ml) was added, the samples were mixed, and radioactivity was quantitated by liquid scintillation spectrometry. Radiochromatograms were sprayed with EN (3)HANCE (DuPont/NEN) and exposed for 2–3 days.

Caspase-3 assay

Caspase-3 activity was assayed by DEVD-AFC cleavage, using the ApoAlert Caspase-3 assay kit (Clontech, Palo Alto, Calif). The assay was performed as described previously (10). Cells were seeded in 100-mm dishes (5×10^6 cells per dish) in 10% FBS RPMI 1640 medium. After 24 h, cells were shifted to 5% FBS RPMI 1640 medium without or with adriamycin and grown for an additional 24 or 48 h. After harvest, cells (10^6 per vial) were lysed (50 μ l lysis buffer on ice, 10 min), and cell debris was removed by centrifugation (4°C, 10,000 g, 5 min). The soluble fraction was incubated with 50 μ M conjugated substrate DEVD-AFC in a 100 μ l reaction volume at 37°C, for 60 min. The free AFC fluoresce was measured at $\lambda_{\text{excitation}}$ 400 nm and $\lambda_{\text{emission}}$ 505 nm using a FL600 Microplate Fluores-

cence Reader. The caspase-3 inhibitor, acetyl-Asp-Glu-Val-Asp-aldehyde was used to exclude nonspecific background in the enzymatic reaction.

Western blot analysis

Western blots were performed using a modified procedure (9, 10, 19). Confluent cell monolayers were washed twice with PBS containing 1.0 mM PMSF and detached with trypsin-EDTA solution. Cells, pelleted by centrifugation, were solubilized in 1.0 ml cold TNT buffer (20 mM Tris-HCl, pH 7.4, 200 mM NaCl, 1.0% Triton X-100, 1.0 mM PMSF, 1.0% aprotinin) for 60 min with shaking. Insoluble debris was excluded by centrifugation at 12,000 g for 45 min at 4°C. The detergent soluble fraction was loaded in equal aliquots, based on protein concentration, and resolved using 4–20% gradient SDS-PAGE. The transferred blot was blocked (3% fat-free milk powder in 10 mM Tris-HCl, pH 8.0, 150 mM NaCl, 0.05% Tween-20) and immuno-blotted with GCS antiserum (1:1000) in binding solution (0.5% BSA in 10 mM Tris-HCl, pH 8.0, 150 mM NaCl) at 4°C for 18 h. To detect Xpress tag and P-glycoprotein, the antibodies of anti-Xpress tag (1:500) and C219 (5 μ g/ml) were used in place of GCS antiserum. Detection using enzyme-linked chemiluminescence was performed using ECL (Amersham).

Rhodamine assay

The rhodamine assay, as a functional test for P-glycoprotein efflux activity, was performed as described previously, with modification (20, 21). MCF-7 cell variants were harvested using trypsin and washed with RPMI 1640 medium. Cells, 2.5×10^6 in 1.0 ml 5% FBS RPMI 1640 medium, were incubated with rhodamine-123 (0.1 mg/ml) for 30 min at 37°C. After centrifugation at 500 g for 15 min, supernatants were discarded, and the cells were washed twice in RPMI 1640 medium. Uptake of rhodamine-123 was measured by adding 200 μ l culture medium containing 0.02% SDS to the cells, and fluorescence was measured at $\lambda_{\text{excitation}}$ 485 nm/ $\lambda_{\text{emission}}$ 530 nm using the FL-600 fluorescent microplate reader. For efflux measurements, 200 μ l of 5% FBS RPMI 1640 medium was added, and the cells were incubated at 37°C for another 60 min. After three washes, cell fluorescence was measured using SDS as above. The efflux was calculated by the difference in cell fluorescence after the 60-min incubation compared with initial cell uptake parameters.

For fluorescence photomicrographs, cells were incubated with 0.1 mg/ml rhodamine-123 in 5% FBS RPMI 1640 medium for 30 min at 37°C. After rinsing, cells were fixed with cold acetic acid/methanol (1:3, v/v) and photomicrographed using an Olympus IX70 fluorescence microscope equipped with a photomicrographic system.

RESULTS

Transfection of GCS sense and antisense cDNA in MCF-7-AdrR cells

Previous work from our laboratory showed that transfection of GCS confers adriamycin resistance in MCF-7 human breast cancer cells (9). MCF-7-AdrR cells, which were selected by treatment of MCF-7 cells with adriamycin, exhibit multidrug resistance (8, 11, 22, 23), have a higher level of GC, and show higher GCS activity compared with MCF-7 cells (3, 8, 11, 24, 25). In the

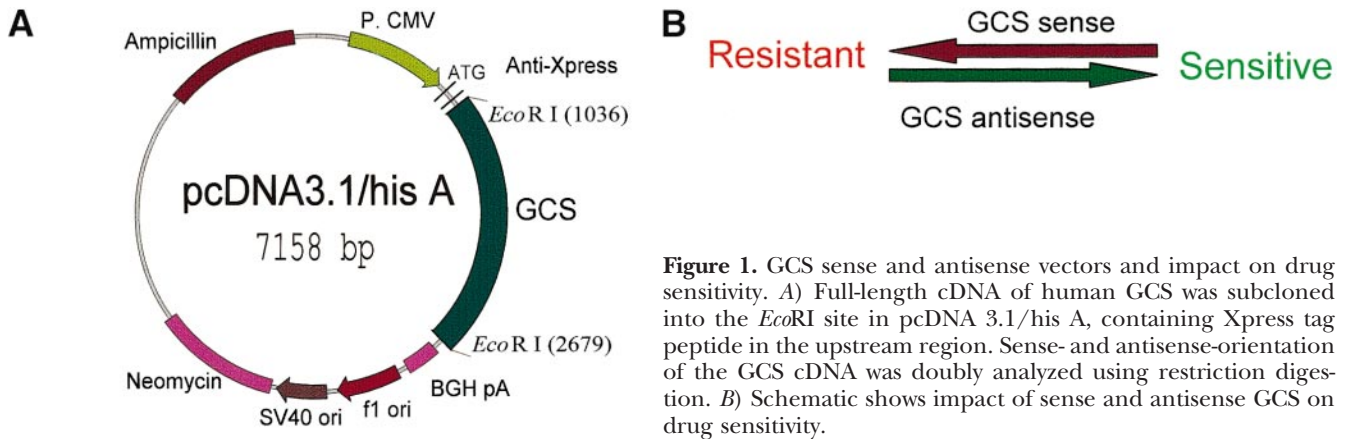


Figure 1. GCS sense and antisense vectors and impact on drug sensitivity. *A*) Full-length cDNA of human GCS was subcloned into the *EcoRI* site in pcDNA 3.1/his A, containing Xpress tag peptide in the upstream region. Sense- and antisense-orientation of the GCS cDNA was doubly analyzed using restriction digestion. *B*) Schematic shows impact of sense and antisense GCS on drug sensitivity.

present study, MCF-7-AdrR cells were transfected with either pcDNA 3.1/his-GCS or pcDNA 3.1/his-asGCS. The full-length GCS (1.7 kb) was excised from pCG-2 (13) and inserted in the *EcoRI* site of pcDNA 3.1/his A (Fig. 1). The orientations of sense and antisense were selected using double restrictive mapping (*HindIII* and *XhoI* plus *NotI*). The pcDNA 3.1/his-GCS was used to develop the MCF-7-AdrR/GCS cell line, and pcDNA 3.1/his-asGCS was used to develop the MCF-7-AdrR/asGCS cell line. As illustrated in Fig. 1 (bottom), because GCS sense confers cellular resistance, it was hypothesized that GCS antisense would sensitize cells to anticancer agents. After co-precipitation with calcium phosphate, the stable expression clones were selected using G-418 and screened using the GCS *in vitro* radioenzymatic assay. We found that the number of G418-resistant clones in MCF-7-AdrR asGCS-transfected cells was much lower ($54/10^6$), compared with MCF-7-AdrR cells transfected with pcDNA3.1/his A ($251/10^6$) or pcDNA3.1/his-GCS vectors ($240/10^6$). Among these clones, Clone 8 in pcDNA3.1/his-GCS transfected MCF-7-AdrR cells stably displayed the highest GCS activity, and Clone 30 in pcDNA3.1/his-asGCS transfected cells exhibited the lowest GCS activity when assayed in more than four different experiments. Another six antisense-transfected clones displayed a 5–20% reduction in GCS activity, compared with empty-vector transfected MCF-7-AdrR clones. Clone 8 was designated MCF-7-AdrR/GCS, and Clone 30 was designated MCF-7-AdrR/asGCS cells. Cells at passages 5–16 were used in the experiments.

MCF-7-AdrR/GCS cells expressed higher GCS levels as measured by RT-PCR, Western blotting, and radioenzymatic assays, compared with MCF-7-AdrR cells (Fig. 2, see Fig. 3). MCF-7-AdrR/GCS cells expressed 168% greater mRNA levels as shown by RT-PCR (Fig. 2A). Western blot analysis using anti-Xpress antibody showed a strong GCS-Xpress tag band in MCF-7-AdrR/GCS cells (Fig. 2B, middle). GCS protein in MCF-7-AdrR/GCS (Fig. 2C, middle) was likewise greater (145%) than that of MCF-7-AdrR cells (Fig. 2C, left). GCS *in vitro* enzyme activity in MCF-7-AdrR/GCS cells was 184% greater compared with the parent cell line, MCF-7-AdrR, or the empty vector (TC) transfected cells (50.5 ± 3.1 vs. 27.37 ± 2.2 pmol GC/h/ μ g protein,

$P < 0.001$, Fig. 3A). Collectively, these data clearly demonstrate that the GCS-transfected cell line MCF-7-AdrR/GCS expresses higher levels of GCS.

MCF-7-AdrR/asGCS cells showed lower levels of GCS compared with parent MCF-7-AdrR cells. MCF-7-AdrR/asGCS cells expressed 30% lower mRNA (Fig. 2A). In Western blots, using anti-Xpress antibody, we did not find a GCS-Xpress tag band in MCF-7-AdrR/asGCS cells (Fig. 2B, right) but rather a higher molecular weight form of Xpress-tag. As shown by Western blot, using GCS antibody, 50% less GCS protein was present in MCF-7-AdrR/asGCS cells (Fig. 2C, right). GCS *in vitro* enzyme activity in MCF-7-AdrR/asGCS cells was 30% lower (19.7 ± 1.0 vs. 27.37 ± 2.2 pmol GC/h/ μ g protein, $P < 0.001$, Fig. 3A) compared with parent cells or empty-vector transfection controls. These results indicate that the expressed GCS antisense mRNA effectively reduces GCS translation and GCS activity in MCF-7-AdrR/asGCS cells.

The morphology of the three cell lines is shown in Fig. 3B. MCF-7-AdrR/GCS cells are more globular, growing in clusters. MCF-7-AdrR/asGCS cells, including the nuclei, are flatter and larger compared with the dome-shaped, more stellate MCF-7-AdrR cells. The MCF-7-AdrR/asGCS cell line is also cuboidal with less dense cytoplasm compared with MCF-7-AdrR cells, and the cells have a lower nucleus/cytoplasm ratio compared with the other cell lines. The population doubling times for three cell lines were similar: 32, 30, and 30 h for MCF-7-AdrR/asGCS, MCF-7-AdrR/GCS, and MCF-7-AdrR cells, respectively.

Anticancer drug response of MCF-7-AdrR, AdrR/GCS, and AdrR/asGCS cells

GCS transfection upgraded resistance to adriamycin and other antineoplastic drugs in MCF-7-AdrR cells, a well known multidrug-resistant cell line (8, 11, 22–25) that displays high levels of GC (3). As shown in Fig. 4A, viability of MCF-7-AdrR/GCS cells was significantly higher than MCF-7-AdrR cells when exposed to increasing concentrations of adriamycin ($P < 0.01$). GCS-transfected cells were threefold more resistant to adriamycin compared with MCF-7-AdrR cells (EC_{50} , 37.3 vs. 12.4

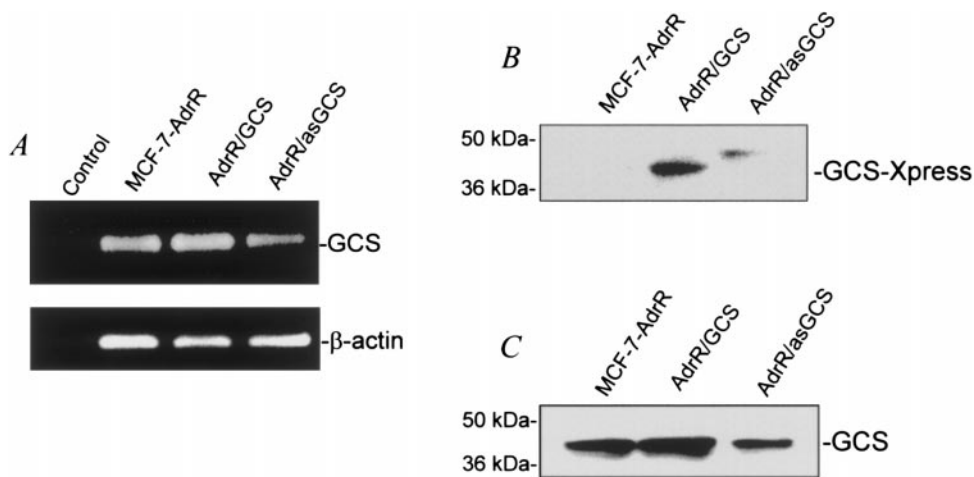


Figure 2. Expression of GCS mRNA and protein. *A*) mRNA expression of GCS by RT-PCR. Isolated mRNA (5 ng) was amplified by high-fidelity RT-PCR and analyzed by 1% agarose gel electrophoresis, stained with ethidium bromide (top strip). β -actin was used as control for even loading (bottom strip). The $OD_{GCS}/OD_{\beta-actin}$ values are MCF-7-AdrR, 0.95; AdrR/GCS, 1.60; AdrR/asGCS, 0.56. Control lane, RT-PCR product without cellular mRNA. AdrR/GCS, MCF-7-AdrR/GCS cells; AdrR/as GCS, MCF-7-AdrR/asGCS cells. *B*) GCS-Xpress Western blot. The detergent soluble fraction (50 μ g protein per lane) was resolved using 4–20% gradient SDS-PAGE. The transferred nitrocellulose blot was blocked (3% fat-free milk powder) and immunoblotted with anti-Xpress antibody (1:1,000). Detection using enzyme-linked chemiluminescence was performed using ECL (Amersham). OD values (densitometry) of GCS-Xpress are MCF-7-AdrR, 7,861; AdrR/GCS, 122,407; AdrR/asGCS, 7,860. *C*) GCS protein in MCF-7-AdrR cells and transfectants. GCS antiserum was used at a 1:1000 dilution. OD values of GCS densitometry for quantitative analysis yielded MCF-7-AdrR, 206,712; AdrR/GCS, 298,368; AdrR/asGCS, 110,808; AdrR/GCS, MCF-7-AdrR/GCS cells; AdrR/asGCS, MCF-7-AdrR/asGCS cells.

μ M, **Table 1**) and twofold more resistant to daunorubicin (EC_{50} , 1.7 vs. 0.9 μ M) and actinomycin D (EC_{50} , 0.15 vs. 0.08, Table 1, Fig. 4). However, an increase in cellular resistance to other anthracyclines, *Vinca* alkaloids, taxanes, or cisplatin did not accompany GCS transfection (Table 1). As hypothesized, transfection of GCS effectively upgraded MCF-7-AdrR cellular resistance to several natural product chemotherapeutic agents, including adriamycin, daunorubicin, and actinomycin D.

In contrast, the antisense-transfected model, MCF-7-AdrR/asGCS, displayed a marked increase in sensitivity

to several different classes of anticancer drugs. As shown in Fig. 4, MCF-7-AdrR/asGCS cell viability in response to adriamycin treatment was significantly reduced compared with MCF-7-AdrR cells, even at concentrations as low as 0.5 μ M ($P < 0.001$), where survival dropped below 50%. Adriamycin sensitivity in antisense transfected cells increased 28-fold (Table 1). The EC_{50} of adriamycin in MCF-7-AdrR/asGCS was 0.44 versus 12.4 μ M in MCF-7-AdrR and 37 μ M in MCF-7-AdrR/GCS cells. For comparison from previous studies, the EC_{50} of adriamycin in MCF-7 cells was 0.37 μ M (9). Thus, GCS antisense transfection of MCF-7-AdrR cells

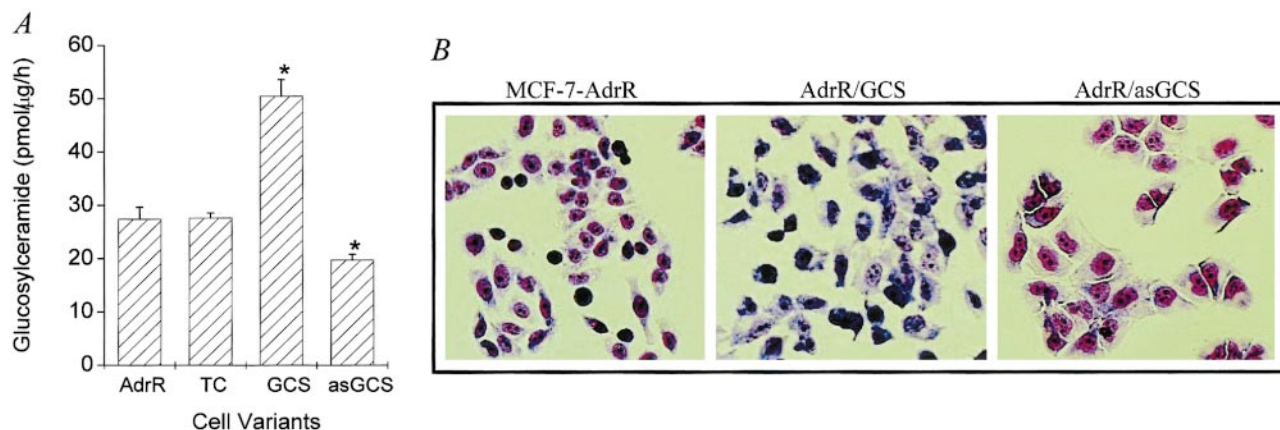
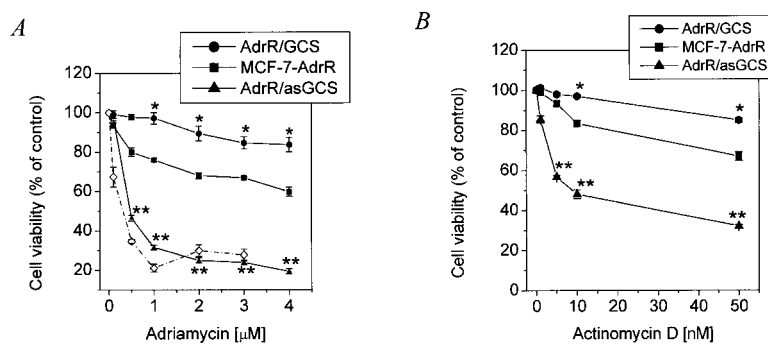


Figure 3. Glucosylceramide synthase activity and morphology of MCF-7-AdrR, MCF-7-AdrR/GCS, and MCF-7-AdrR/asGCS cells. *A*) GCS activity. Enzyme activity was measured as detailed in Materials and Methods. Data represent the mean \pm SD of three replicates from three independent experiments. $*P < 0.001$ compared with MCF-7-AdrR cells. AdrR, MCF-7-AdrR cells; TC, transfection control (MCF-7-AdrR cells transfected with pcDNA 3.1 vector alone); GCS, MCF-7-AdrR/GCS cells; asGCS, MCF-7-AdrR/asGCS cells. *B*) Comparison of cell morphology in MCF-7-AdrR and GCS transfectants. After 48 h of subculture, cells were stained using the May-Grunwald-Giemsa method and photographed at 200 \times magnification.

Figure 4. Toxicity of adriamycin and actinomycin D in MCF-7-AdrR, MCF-7-AdrR/GCS, and MCF-7-AdrR/asGCS cells. A) Adriamycin toxicity. Cells were treated with adriamycin at increasing concentrations in 5% FBS RPMI 1640 medium. After 72-h exposure, adriamycin cytotoxicity was determined using the Promega 96 Aqueous cell proliferation assay kit. \diamond — \diamond Adriamycin toxicity in MCF-7 cells. B) Actinomycin D toxicity. Cells were treated as in panel A, except adriamycin was replaced with actinomycin D. Data represent the mean \pm SD of six replicates from three independent experiments. * P < 0.001, ** P < 0.0001 compared with MCF-7 AdrR cells.



restored adriamycin sensitivity to the level displayed by MCF-7 cells. MCF-7-AdrR/asGCS cells were also 11- and 7-fold more sensitive to daunorubicin (EC_{50} , 0.08 vs. 0.91 μ M) and idarubicin (EC_{50} , 0.06 vs. 0.42 μ M), respectively, compared with MCF-7-AdrR cells (Table 1). Interestingly, GCS antisense transfection markedly potentiated cellular sensitivity to *Vinca* alkaloids, taxanes, and actinomycin D. The degree of increased sensitivity to taxol and vinblastine in GCS antisense cells is shown in **Fig. 5A, B**, respectively. GCS antisense transfection diminished the cytotoxic threshold of taxol and vinblastine from the micromolar to nanomolar range. Cellular sensitivity to vinblastine, vincristine, taxol, taxotere, and actinomycin D increased by 115-, 50-, 241-, 66-, and 9-fold, respectively (Table 1). In contrast, sensitivity to 5-fluorouracil increased only 3.6-fold in MCF-7-AdrR/asGCS cells, and the EC_{50} of cisplatin in the three cell lines remained unchanged (Table 1). These data demonstrate that the expression of GCS antisense reverses multidrug resistance, and that reversal is specific for certain drug classes.

Colony formation in soft agar under drug-free conditions was also evaluated, and a difference in the three cell lines was not demonstrated. However, under adriamycin stress, GCS sense cDNA transfectants exhibited enhanced colony formation (**Fig. 6**), whereas GCS

antisense cDNA transfectants showed a marked decrease in colony formation (**Fig. 6**). With 2.5 μ M adriamycin, colony formation was <10% in MCF-7-AdrR/asGCS cells, compared with 70% in MCF-7-AdrR and 99% in MCF-7-AdrR/GCS cells. Thus, adriamycin toxicities in the GCS antisense-transfected cells were on a par, whether treated under anchorage-dependent (Table 1) or anchorage-independent growth conditions (**Fig. 6**).

Resumption of ceramide signal in MCF-7-AdrR/asGCS cells potentiates drug cytotoxicity

To further elucidate the dynamics of ceramide metabolism in anthracycline sensitivity, we measured ceramide generation in the three cell lines and found that adriamycin elevated ceramide levels in GCS antisense transfected cells. As shown in **Fig. 7A**, adriamycin at 0.5 μ M increased the levels of ceramide in MCF-7-AdrR/asGCS cells by 184% compared with MCF-7-AdrR cells (632 ± 67 vs. 344 ± 25 cpm) and 227% (857 ± 24 vs. 376 ± 16 cpm) at 2.5 μ M (P < 0.001). In contrast, MCF-7-AdrR/GCS cells did not display a ceramide response when challenged with adriamycin (**Fig. 7A**). Another

TABLE 1. Influence of GCS transfection on chemotherapy sensitivity in drug-resistant MCF-7-AdrR cells

	MCF-7-AdrR		MCF-7-AdrR/GCS		MCF-7-AdrR/asGCS	
	EC_{50} (μ M)		EC_{50} (μ M)	R. Index	EC_{50} (μ M)	S. Index
Adriamycin	12.4 \pm 0.68		37.3 \pm 1.89*	3	0.44 \pm 0.01*	28
Daunorubicin	0.91 \pm 0.09		1.73 \pm 0.06*	2	0.08 \pm 0.0*	11
Idarubicin	0.42 \pm 0.0		0.45 \pm 0.01	1	0.06 \pm 0.01*	7
Epirubicin	9.30 \pm 0.30		10.0 \pm 0.1	1	4.30 \pm 0.06*	2
Vinblastine	0.73 \pm 0.01		0.46 \pm 0.01	0.6	0.006 \pm 0.000*	115
Vincristine	2.14 \pm 0.03		1.40 \pm 0.14	0.6	0.05 \pm 0.0001*	50
Taxol	3.38 \pm 0.06		2.75 \pm 0.06	0.8	0.014 \pm 0.0002*	241
Taxotere	4.65 \pm 0.19		3.91 \pm 0.06	0.9	0.07 \pm 0.01*	66
Actinomycin D	0.083.00 \pm 0.008		0.145 \pm 0.006*	1.7	0.009 \pm 0.001*	9
5-Fluorouracil	49.5 \pm 1.29		54.5 \pm 1.29	1	13.5 \pm 1.29*	3.6
Cisplatin	4.04 \pm 0.09		3.38 \pm 0.15	1	3.4 \pm 0.14	1

The EC_{50} (concentration of drug affecting a 50% kill) for each drug tested is listed for each of the three cell lines. In GCS-sense transfected cells, MCF-7-AdrR/GCS, enhanced drug resistance is shown by "R. Index" (Resistance Index) and is designated numerically by fold increase in drug EC_{50} compared with MCF-7-AdrR cells. In GCS-antisense transfected cells, MCF-7-AdrR/asGCS, enhanced drug sensitivity is shown by "S. Index" (Sensitivity Index) and is designated numerically by fold decrease in drug EC_{50} , compared with MCF-7-AdrR cells. The EC_{50} of adriamycin in MCF-7 cells is 0.37 μ M(10). * P < 0.001, compared with MCF-7-AdrR cells.

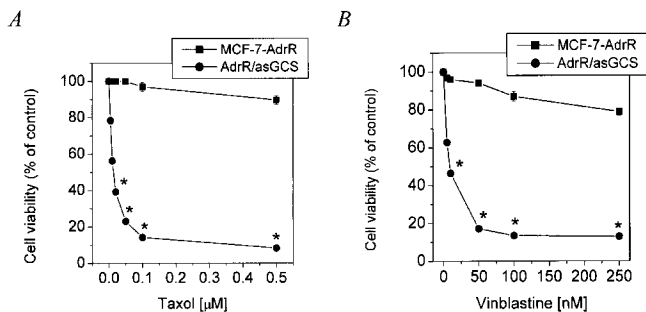


Figure 5. Influence of GCS antisense transfection on taxol and vinblastine sensitivity. *A*) Taxol sensitivity. Cells were treated with taxol at increasing concentrations in 5% FBS RPMI 1640 medium. After 72-h exposure, taxol cytotoxicity was determined using the Promega 96 Aqueous cell proliferation assay kit. *B*) Vinblastine sensitivity. Cells were treated as in panel A, except taxol was replaced with vinblastine. Data represent the mean \pm SD of six replicates from three independent experiments. * $P < 0.0001$ compared with MCF-7-AdrR cells under the same conditions.

agent, actinomycin D, also potentiated cellular ceramide generation in GCS antisense transfected cells (Fig. 7B), with no significant changes occurring in either MCF-7-AdrR or MCF-7-AdrR/GCS cells.

We next examined GC levels in the three cell lines under basal conditions and under adriamycin exposure. As shown in Fig. 8A by TLC autoradiography, GCS antisense transfection reduced cellular levels of GC (lane 3), compared with MCF-7-AdrR cells (lane 1). When evaluated by scintillation spectroscopy, MCF-7-AdrR/asGCS cells exhibited an $\sim 27\%$ decrease in GC compared with parent cells (1854 ± 54 vs. 2546 ± 133 cpm, Fig. 8B, minus adriamycin). GC was slightly elevated in GCS sense transfectants (Fig. 8A, lane 2); however, the difference was not statistically significant compared with MCF-7-AdrR cells (2819 ± 174 vs. 2546 ± 133 cpm, Fig. 8B, minus adriamycin). Although adriamycin exposure elicits ceramide increases in MCF-7-AdrR/asGCS cells (Fig. 7A), exposure to this drug did not alter GC metabolism in any of the cell lines (Fig. 8B).

Increases in effector caspase activity in ceramide-governed apoptotic signaling are consistent with changes in ceramide levels. With 10μ M adriamycin (EC_{50} in MCF-7-AdrR cells), caspase-3 activity in MCF-

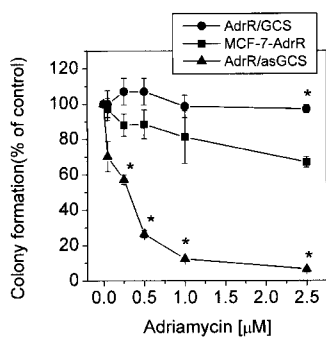


Figure 6. Influence of adriamycin on colony formation under anchorage-independent conditions in MCF-7-AdrR and GCS transfectants. Cells were treated with the indicated concentration of adriamycin for 120 h, and colony formation was analyzed by [3 H]thymidine incorporation. Data represent the mean \pm SD of triplicates from three independent experiments. * $P < 0.01$, compared with MCF-7-AdrR cells.

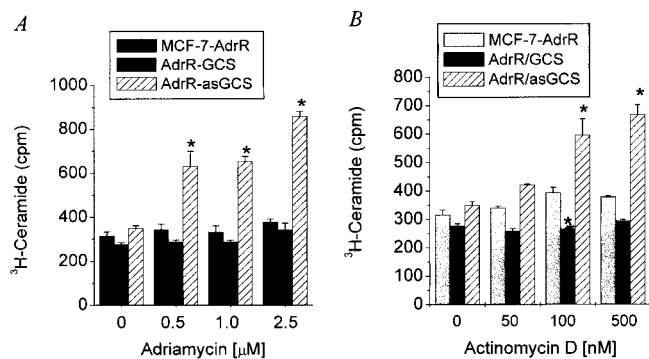


Figure 7. Ceramide generation in response to adriamycin and actinomycin D. Cellular lipids were radiolabeled by incubating cells with [3 H]palmitic acid (2.5μ Ci/ml culture medium) for 24 h, and total lipids were extracted for analysis. Ceramide was resolved by TLC. Ceramide values are given as cpm per 10^5 cpm total lipid. *A*) Influence of adriamycin dose on cellular ceramide metabolism. Cells were treated with the indicated concentrations of adriamycin for 48 h. *B*) Influence of actinomycin D dose on cellular ceramide metabolism. Cells were treated with the indicated concentrations of actinomycin D for 48 h. Data represent the mean \pm SD of triplicates from three independent experiments. * $P < 0.001$ compared with MCF-7-AdrR cells under the same conditions.

7-AdrR/asGCS cells increased 3- (1.99 ± 0.005 vs. 0.63 ± 0.005 nmole AFC/ 10^6 cells, $P < 0.001$) and 3.6-fold (3.6 ± 0.04 vs. 1.02 ± 0.03 nmole AFC/ 10^6 cells, $P < 0.001$), at 24- and 48-h treatment, respectively, compared with MCF-7-AdrR cells (Fig. 9A). Under like conditions, caspase-3 activity in MCF-7-AdrR/GCS cells had no significant decrease, compared with activity in

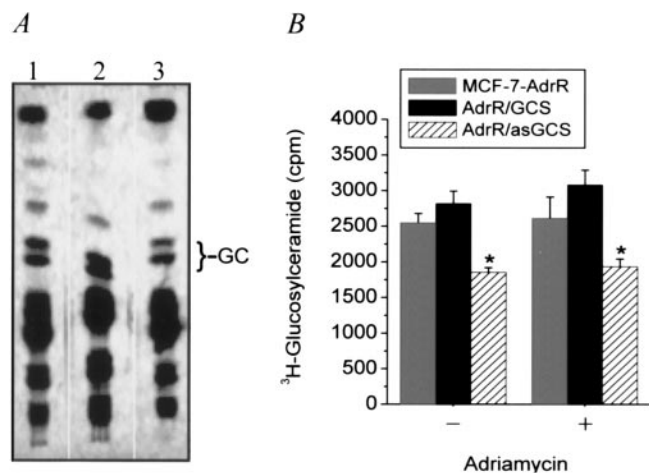


Figure 8. Cellular glucosylceramide metabolism in response to adriamycin treatment. Cellular lipids were radiolabeled by incubating cells with [3 H]palmitic acid (2.5μ Ci/ml culture medium) for 24 h. Total lipids were extracted and GC was resolved by TLC. GC values are given as cpm per 10^5 cpm total lipid. *A*) GC TLC autoradiograph. Lanes 1, 2, and 3 show total lipids from MCF-7-AdrR, MCF-7-AdrR/GCS and MCF-7-AdrR/asGCS cells, respectively. *B*) Influence of adriamycin on cellular GC metabolism. Cells were treated with adriamycin (2.0μ M) for 48 h. Data represent the mean \pm SD of triplicates from two independent experiments. * $P < 0.01$ compared with MCF-7-AdrR cells under the same conditions.

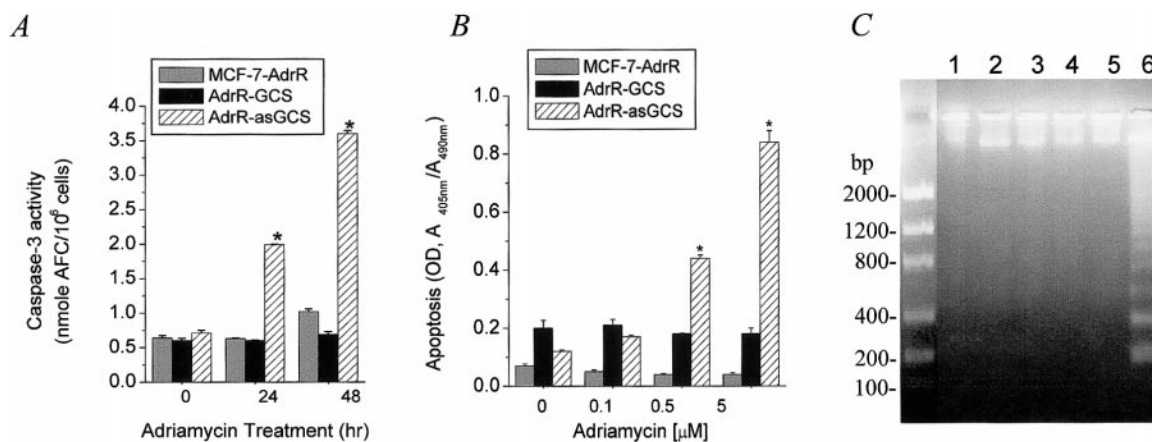


Figure 9. Caspase-3 activity and apoptosis in response to adriamycin in MCF-7 GCS transfectants. *A*) Caspase-3 activity. Cells were treated without or with adriamycin (10 μ M) for 24 and 48 h. Data represent the mean \pm SD of triplicates from two independent experiments. * $P < 0.0001$ compared with MCF-7-AdrR cells exposed to adriamycin for each corresponding treatment period. *B*) Apoptosis. Cells were treated without or with the indicated concentrations of adriamycin for 48 h. Data represent the mean \pm SD of triplicates from two independent experiments. * $P < 0.0001$ compared with MCF-7-AdrR cells exposed to adriamycin for each corresponding treatment period. *C*) DNA fragmentation. Cells were exposed to 5.0 μ M adriamycin for 72 h, and cellular DNA was extracted and resolved by 2% agarose gel electrophoresis. Left lane, low DNA mass ladder standard. Lanes 1, 3, 5 show MCF-7-AdrR, MCF-7-AdrR/GCS and MCF-7-AdrR/asGCS cells, respectively. Lanes 2, 4, 6 show MCF-7-AdrR, MCF-7-AdrR/GCS and MCF-7-AdrR/asGCS cells treated with 5.0 μ M adriamycin, respectively.

MCF-7-AdrR cells at 48 h. Further characterization revealed that adriamycin elicited apoptosis only in the GCS antisense-transfected cells (Fig. 9B, C). The levels of apoptosis in GCS antisense cells increased with increasing concentration of adriamycin. The apoptotic index was 370 (0.44 ± 0.01 vs. 0.12 ± 0.005 OD) and 700% (0.84 ± 0.04 vs. 0.12 ± 0.005 OD) of untreated MCF-7-AdrR/asGCS cells at 0.5 and 5.0 μ M adriamycin, respectively (Fig. 9B). Using DNA fragmentation analysis, adriamycin treatment (5.0 μ M, 72 h) only induced apoptosis in MCF-7-AdrR/asGCS cells (Fig. 9C, lane 6). Overall, these data show that reduced glycosylation potential enhances cellular buildup of free ceramide under adriamycin stress and potentiates the progression of programmed cell death via caspase.

P-glycoprotein expression and efflux parameters

P-glycoprotein-modulated drug efflux is the most widely characterized drug resistance mechanism (26), and it is highly expressed in MCF-7-AdrR cells (9, 22). However, adriamycin resistance produced by enforced expression of GCS is not accompanied by increased P-glycoprotein in MCF-7/GCS cells (9). To assess the role of the *MDR1* phenotype in enhanced drug sensitivity expressed by GCS antisense transfectants, we analyzed rhodamine-123 efflux and P-glycoprotein expression in the MCF-7 cell variants (Fig. 10). Enhanced rhodamine-123 efflux was observed in all cell lines, except MCF-7 (Fig. 10A). The enhanced efflux correlated with overexpression of P-glycoprotein in the MCF-7-AdrR cell variants (Fig. 10B). Therefore, the up- or down-regulation of GCS activity by transfection had little influence on either rhodamine-123 efflux or P-glycoprotein expression (Fig. 10A, B). This suggests

that P-glycoprotein is not a major mechanism involved in chemotherapy sensitization that accompanies GCS antisense transfection. Interestingly, we found enhanced uptake of rhodamine-123 in MCF-7-AdrR/asGCS cells, compared with MCF-7-AdrR and MCF-7-AdrR/GCS cells. The degree of enhancement was similar with the fluorescence intensity observed in wild-type MCF-7 cells (Fig. 11A). Quantitative fluorescence measurement of intracellular rhodamine-123 showed that MCF-7 cells took up 41% of the total ($7,043 \pm 57/1.7 \times 10^4$ FU, [fluorescence units]) on a parallel with MCF-7-AdrR/asGCS (41%, $7,077 \pm 518/$

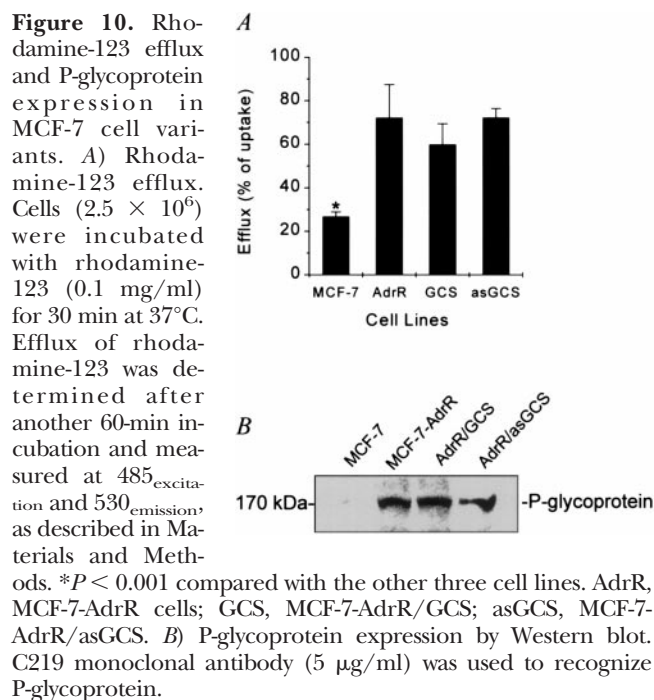


Figure 10. Rhodamine-123 efflux and P-glycoprotein expression in MCF-7 cell variants. *A*) Rhodamine-123 efflux. Cells (2.5×10^6) were incubated with rhodamine-123 (0.1 mg/ml) for 30 min at 37°C. Efflux of rhodamine-123 was determined after another 60-min incubation and measured at 485_{excitation} and 530_{emission}, as described in Materials and Methods. * $P < 0.001$ compared with the other three cell lines. AdrR, MCF-7-AdrR cells; GCS, MCF-7-AdrR/GCS; asGCS, MCF-7-AdrR/asGCS. *B*) P-glycoprotein expression by Western blot. C219 monoclonal antibody (5 μ g/ml) was used to recognize P-glycoprotein.

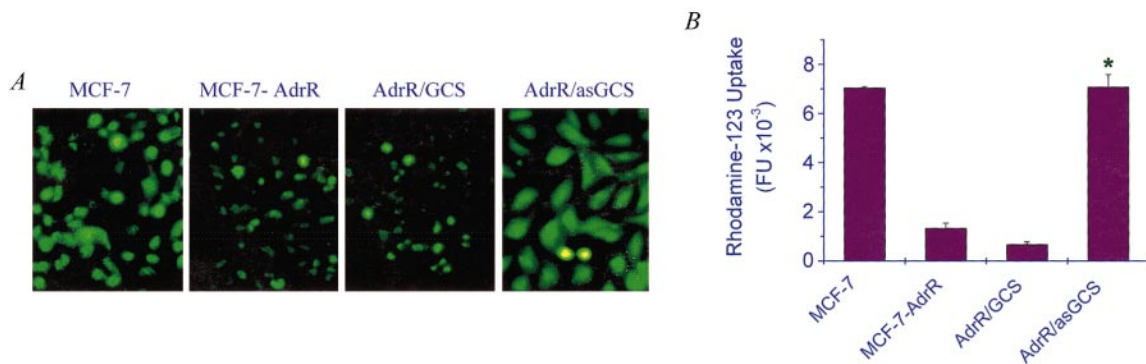


Figure 11. Rhodamine-123 uptake in MCF-7 cell variants. A) Fluorescence photomicrographs of MCF-7 cell variants after incubation with rhodamine-123. Cells were incubated with rhodamine-123 (0.1 mg/ml) for 30 min at 37°C and fixed as detailed in Materials and Methods. B) Cellular uptake of Rhodamine-123. Cells (2.5×10^6) were incubated with rhodamine-123 (0.1 mg/ml) for 30 min at 37°C. After washing, uptake of rhodamine-123 was determined in the SDS-lysate, by fluorescence, as described in Materials and Methods. * $P < 0.001$ compared with MCF-7-AdrR cells.

1.7×10^4 FU). Rhodamine-123 uptake in GCS antisense transfectants was fivefold greater than uptake in MCF-7-AdrR cells ($7,077 \pm 518$ vs. $1,331 \pm 213$ FU) and 10-fold greater than uptake in MCF-7-AdrR/GCS cells ($7,077 \pm 518$ vs. 669 ± 106 FU) (Fig. 11B).

DISCUSSION

MCF-7-AdrR cells exhibit cross-resistance to a wide range of antineoplastic agents including *Vinca* alkaloids, anthracyclines, and epipodophyllotoxins (12, 22, 23). Although there is overexpression of P-glycoprotein and glutathione-S-transferase in MCF-7-AdrR cells (22, 27), there have been no reports showing that antisense transfection with either P-glycoprotein or glutathione-S-transferase reverses multidrug resistance in these cells. Our study shows that drug resistance can be reversed by antisense manipulation of ceramide metabolism, and the work reinforces the doctrine that drug resistance in cancer is multifactorial (28).

Through gene targeting, it has been shown that GCS sense cDNA transfection induces resistance to adriamycin by 11-fold in MCF-7 cells (9). Although MCF-7-AdrR cells constitutively display high GCS activity and elevated GC levels (3, 8), introducing GCS cDNA into these multidrug-resistant cells upgraded, albeit only severalfold, the resistance threshold for adriamycin (Fig. 4, Table 1), daunorubicin, and actinomycin D (Table 1). Compared with MCF-7 cells, the high basal levels of GC (sixfold more) and enhanced GCS enzyme activity (8), which contribute to multidrug resistance, may interfere with the efficacy of GCS transfection for further enhancement of drug resistance in MCF-7-AdrR cells. On the other hand, GCS antisense, which effectively reintroduced ceramide/caspase signaling (Figs. 7 and 8), substantially restored cellular sensitivity to many anticancer drugs, including anthracyclines, taxanes, *Vinca* alkaloids, and actinomycin D (Table 1). All of these agents are substrates for P-glycoprotein (26), whereas 5-fluorouracil and cisplatin, whose toxicities

were not greatly modified by GCS antisense, are not classified as pump drugs. This raises the question of selectivity of GCS antisense for reversal of drug resistance, a topic that is currently being pursued. GCS antisense also sensitized cells that were grown in soft agar to adriamycin (Fig. 5) and sensitized cells grown under hypoxic conditions ($O_2 < 5\%$, data not shown). These results suggest that GCS antisense is promising for restoring drug sensitivity under conditions that mimic tumor *in vivo* environments. Overall, these data indicate that GCS is a cause of multidrug resistance in MCF-7 breast cancer cells.

Overexpression of P-glycoprotein reduces intracellular accumulation of chemotherapeutic agents and produces multidrug resistance (26, 29). However, the role that P-glycoprotein exerts in breast cancer has been difficult to define (30–32). Kim et al. reported that P-glycoprotein (*MDR-1*) is a minor determinant of drug resistance in MCF-7-AdrR cells (32). We did not observe increased P-glycoprotein expression in MCF-7/GCS cells in which adriamycin resistance was induced by GCS overexpression (9). We also did not observe decreased expression of P-glycoprotein in MCF-7-AdrR/asGCS cells. When we analyzed rhodamine-123 efflux and P-glycoprotein expression in MCF-7 cell lines (Fig. 8), our observations were much in line with previous work showing that MCF-7-AdrR cells have an enhanced efflux capacity, complementing the enhanced levels of P-glycoprotein (12, 22, 23). Although GCS antisense transfection sensitized resistant cells to several different types of drugs, antisense did not modulate either P-glycoprotein expression or efflux parameters. This suggests that P-glycoprotein is not the major mechanism involved in chemotherapy sensitization that accompanies GCS antisense transfection.

Ceramide is a lipid second messenger in the apoptotic pathway, participating in cell death initiated by anticancer drugs, cytokines, and ionizing radiation (33, 34). The apoptotic impact of adriamycin, daunorubicin, and actinomycin D depends, in part, on cellular ceramide generation (9, 24, 35, 36). Increased cer-

amide levels enhance the efficacy of vinblastine (37) and taxol (38). In this study, we show that impairment of ceramide glycosylation increases intracellular ceramide levels and propels apoptotic signaling in response to antineoplastic drugs. In addition to glycosylation, ceramide can be converted to sphingomyelin (via sphingomyelin synthase), galactosylceramide (via galactosylceramide synthase), or undergo deacylation to form sphingosine (via ceramidase) (39). However, as a route to remove ceramide, up-regulating the conversion of ceramide to sphingomyelin, through sphingomyelin synthase, may be harmful to the cell, as the levels of sphingomyelin are tightly regulated. Therefore, although sphingomyelin synthase regulates intracellular ceramide levels (40), GCS appears to be more influential over cell growth and apoptosis. GCS converts cytotoxic ceramide to GC, an essential building block of more complex cell membrane components. Various works show that GC stimulates cell proliferation (41, 42) and tumor growth (43, 44), whereas GCS inhibitors arrest cell division (45, 46), exhibit anticarcinogenic properties (46), and reduce metastasis (47). Complex derivatives of GC, such as gangliosides GM₃, GM₂, and GD₂, are also involved in cell growth, tumor metastasis, and drug resistance (48–50). Therefore, lowering glycosphingolipid synthesis by modifying GC metabolism appears to be a novel strategy in cancer chemotherapy (10, 51–53).

In the present study, GCS antisense markedly sensitized breast cancer cells to several well-known antitumor agents. Taking into account the 30% decrease in GCS activity in MCF-7-AdrR/asGCS cells (Fig. 3), multifold increases in sensitivity to the various drugs (Table 1) are striking. In addition to modulating cellular ceramide and GC levels under stress, GCS catalyzes the first glycosylation step in the biosynthesis of glycosphingolipids, lipids which are present on virtually all mammalian cell plasma membranes (54, 55). Glycosphingolipids are integral components of plasma membrane microdomains, such as rafts, caveolae, and GM₃-enriched microdomains (56, 57). Microdomains are involved in drug resistance (58, 59), mediating membrane trafficking and signal activity, and coupling cell adhesion interactions with signaling (60, 61). A GCS knockout study in mice showed that the consequence of homozygosity was embryonic lethality, revealing a vital role for GCS during development and differentiation (62). Lowering GCS by 1-phenyl-2-decanoylamino-3-morpholino-propanol exposure brings about morphological change in Chinese hamster ovary cells (63), in cultured cortical neuron (64), and in PC12 cells (65). Ganglioside, GQ1b, is essential for synapse formation and synaptic activity (64). We also found GCS antisense cDNA markedly altered MCF-7-AdrR cell morphology (Fig. 2) and greatly increased the uptake of rhodamine-123 (Fig. 10). This suggests that alteration of membrane glycosphingolipid composition, by enforced expression of GCS antisense, effects cell morphology and membrane functional activities, including drug transport. Enhanced drug import, which may

partially underlie the increased sensitivity to anticancer drugs observed in MCF-7-AdrR/asGCS cells, is being further investigated. FJ

This work was supported in part by a PHS grant from the National Cancer Institute (CA77632); The Streisand Foundation; the Strauss Foundation, Sandra Krause, Trustee; the Fashion Footwear Association of New York, FFANY; the Associates for Breast and Prostate Cancer Studies, Los Angeles; the Leslie and Susan Gonda (Goldschmied) Foundation, and the Joseph B. Gould Foundation, Las Vegas, NV. Y. L. is a Joseph B. Gould Fellow in Breast Cancer Research.

We thank Dr. Shinichi Ichikawa and Dr. Yoshio Hirabayashi (Laboratory for Cellular Glycobiology, The Institute of Chemical and Physical Research, RIKEN, Saitama, Japan) for providing the ceramide glucosyltransferase cDNA, pCG 2, and Dr. D. L. Marks and Dr. R. E. Pagano (Mayo Clinic and Foundation) for GCS antiserum. We appreciate the advice of Dr. James Hardin, John Wayne Cancer Institute, in the review of this work.

REFERENCES

- Hannun, Y. A. (1996) Functions of ceramide in coordinating cellular responses to stress. *Science* **274**, 1855–1859
- Kolesnick, R. N., and Kronke, M. (1998) Regulation of ceramide production and apoptosis. *Annu. Rev. Physiol.* **60**, 643–665
- Lavie, Y., Cao, H., Bursten, S. L., Giuliano, A. E., and Cabot, M. C. (1996) Accumulation of glucosylceramides in multidrug-resistant cancer cells. *J. Biol. Chem.* **271**, 19530–19536
- Nicholson, K. M., Quinn, D. M., Kellett, G. L., and Warr, J. R. (1999) Preferential killing of multidrug-resistant KB cells by inhibitors of glucosylceramide synthase. *Br. J. Cancer* **81**, 423–430
- Kok, J. W., Veldman, R. J., Klappe, K., Koning, H., Filipceanu, C. M., and Muller, M. (2000) Differential expression of sphingolipids in MRP1 overexpressing HT29 cells. *Int. J. Cancer* **87**, 172–178
- Lala, P., Ito, S., and Lingwood, C. A. (2000) Retroviral transfection of Madin-Darby canine kidney cells with human MDR1 results in a major increase in globotriaosylceramide and 10⁵- to 10⁶-fold increased cell sensitivity to verocytotoxin: role of p-glycoprotein in glycolipid synthesis. *J. Biol. Chem.* **275**, 6246–6251
- Lucci, A., Cho, W. I., Han, T. Y., Giuliano, A. E., Morton, D. L., and Cabot, M. C. (1998) Glucosylceramide: a marker for multiple-drug resistant cancers. *Anticancer Res.* **18**, 475–480
- Lavie, Y., Cao, H., Volner, A., Lucci, A., Han, T. Y., Geffen, V., Giuliano, A. E., and Cabot, M. C. (1997) Agents that reverse multidrug resistance, tamoxifen, verapamil, and cyclosporin A, block glycosphingolipid metabolism by inhibiting ceramide glycosylation in human cancer cells. *J. Biol. Chem.* **272**, 1682–1687
- Liu, Y. Y., Han, T. Y., Giuliano, A. E., and Cabot, M. C. (1999) Expression of glucosylceramide synthase, converting ceramide to glucosylceramide, confers adriamycin resistance in human breast cancer cells. *J. Biol. Chem.* **274**, 1140–1146
- Liu, Y. Y., Han, T. Y., Giuliano, A. E., Ichikawa, S., Hirabayashi, Y., and Cabot, M. C. (1999) Glycosylation of ceramide potentiates cellular resistance to tumor necrosis factor- α -induced apoptosis. *Exp. Cell Res.* **252**, 464–470
- Liu, Y. Y., Han, T. Y., Giuliano, A. E., Hansen, N., and Cabot, M. C. (2000) Uncoupling ceramide glycosylation by transfection of glucosylceramide synthase antisense reverses adriamycin resistance. *J. Biol. Chem.* **275**, 7138–7143
- Cowan, K. H., Batist, G., Tulpule, A., Sinha, B. K., and Myers, C. E. (1986) Similar biochemical changes associated with multidrug resistance in human breast cancer cells and carcinogen-induced resistance to xenobiotics in rats. *Proc. Natl. Acad. Sci. USA* **83**, 9328–9332
- Ichikawa, S., Sakiyama, H., Suzuki, G., Hidari, K. I., and Hirabayashi, Y. (1996) Expression cloning of a cDNA for human

- ceramide glucosyltransferase that catalyzes the first glycosylation step of glycosphingolipid synthesis. *Proc. Natl. Acad. Sci. USA* **93**, 4638–4643
14. Shukla, G. S., and Radin, N. S. (1990) Glucosylceramide synthesis of mouse kidney: further characterization with an improved assay method. *Arch. Biochem. Biophys.* **283**, 372–378
 15. Jones, C. A., Tsukamoto, T., O'Brien, P. C., Uhl, C. B., Alley, M. C., and Lieber, M. M. (1985) Soft agarose culture human tumour colony forming assay for drug sensitivity testing: [³H]-thymidine incorporation vs colony counting. *Br. J. Cancer.* **52**, 303–310
 16. Chen, J., Bander, J. A., Santore, T. A., Chen, Y., Ram, P. T., Smit, M. J., and Iyengar, R. (1998) Expression of Q227L-galphas in MCF-7 human breast cancer cells inhibits tumorigenesis. *Proc. Natl. Acad. Sci. USA* **95**, 2648–2652
 17. Wyllie, A. H., Kerr, J. F., and Currie, A. R. (1980) Cell death: the significance of apoptosis. *Int. Rev. Cytol.* **68**, 251–306
 18. Bonfoco, E., Krainc, D., Ankarcrona, M., Nicotera, P., and Lipton, S. A. (1995) Apoptosis and necrosis: two distinct events induced, respectively, by mild and intense insults with N-methyl-D-aspartate or nitric oxide/superoxide in cortical cell cultures. *Proc. Natl. Acad. Sci. USA* **92**, 7162–7166
 19. Watanabe, R., Wu, K., Paul, P., Marks, D. L., Kobayashi, T., Pittelkow, M. R., and Pagano, R. E. (1998) Up-regulation of glucosylceramide synthase expression and activity during human keratinocyte differentiation. *J. Biol. Chem.* **273**, 9651–9655
 20. Stein, U., Walther, W., Lemm, M., Naundorf, H., and Fichtner, I. (1997) Development and characterisation of novel human multidrug resistant mammary carcinoma lines in vitro and in vivo. *Int. J. Cancer* **72**, 885–891
 21. Brouty-Boye, D., Kolonias, D., Wu, C. J., Savaraj, N., and Lampidis, T. J. (1995) Relationship of multidrug resistance to rhodamine-123 selectivity between carcinoma and normal epithelial cells: taxol and vinblastine modulate drug efflux. *Cancer Res.* **55**, 1633–1638
 22. Fairchild, C. R., Ivy, S. P., Kao-Shan, C. S., Whang-Peng, J., Rosen, N., Israel, M. A., Melera, P. W., Cowan, K. H., and Goldsmith, M. E. (1987) Isolation of amplified and overexpressed DNA sequences from adriamycin-resistant human breast cancer cells. *Cancer Res.* **47**, 5141–5148
 23. Fairchild, C. R., Moscow, J. A., O'Brien, E. E., and Cowan, K. H. (1990) Multidrug resistance in cells transfected with human genes encoding a variant P-glycoprotein and glutathione S-transferase-pi. *Mol. Pharmacol.* **37**, 801–809
 24. Cabot, M. C., and Giuliano, A. E. (1997) Apoptosis: a cell mechanism important for cytotoxic response to adriamycin and a lipid metabolic pathway that facilitates escape. *Breast Cancer Res. Treat.* **46**, 283
 25. Cabot, M. C., Han, T. Y., and Giuliano, A. E. (1998) The multidrug resistance modulator SDZ PSC 833 is a potent activator of cellular ceramide formation. *FEBS Lett.* **431**, 185–188
 26. Gottesman, M. M., and Pastan, I. (1993) Biochemistry of multidrug resistance mediated by the multidrug transporter. *Annu. Rev. Biochem.* **62**, 385–427
 27. Batist, G., Tulpule, A., Sinha, B. K., Katki, A. G., Myers, C. E., and Cowan, K. H. (1986) Overexpression of a novel anionic glutathione transferase in multidrug-resistant human breast cancer cells. *J. Biol. Chem.* **261**, 15544–15549
 28. Lehnert, M. (1996) Clinical multidrug resistance in cancer: a multifactorial problem. *Eur. J. Cancer* **32A**, 912–920
 29. Riordan, J. R., and Ling, V. (1979) Purification of P-glycoprotein from plasma membrane vesicles of Chinese hamster ovary cell mutants with reduced colchicine permeability. *J. Biol. Chem.* **254**, 12701–12705
 30. Decker, D. A., Morris, L. W., Levine, A. J., Pettinga, J. E., Grudzien, J. L., and Farkas, D. H. (1995) Immunohistochemical analysis of P-glycoprotein expression in breast cancer: clinical correlations. *Ann. Clin. Lab. Sci.* **25**, 52–59
 31. Schneider, J., and Romero, H. (1995) Correlation of P-glycoprotein overexpression and cellular prognostic factors in formalin-fixed, paraffin-embedded tumor samples from breast cancer patients. *Anticancer Res.* **15**, 1117–1121
 32. Kim, H. M., Oh, G. T., Hong, D. H., Kim, M. S., Kang, J. S., Park, S. M., and Han, S. B. (1997) MDR-1 gene expression is a minor factor in determining the multidrug resistance phenotype of MCF7/ADR and KB-V1 cells. *FEBS Lett.* **412**, 201–206
 33. Darvis, W. D., and Grant, S. (1998) The role of ceramide in the cellular response to cytotoxic agents. *Curr. Opin. Oncol.* **10**, 552–559
 34. Radford, I. R. (1999) Initiation of ionizing radiation-induced apoptosis: DNA damage-mediated or does ceramide have a role? *Int. J. Radiat. Biol.* **75**, 521–528
 35. Bose, R., Verheij, M., Haimovitz-Friedman, A., Scotto, K., Fuks, Z., and Kolesnick, R. (1995) Ceramide synthase mediates daunorubicin-induced apoptosis: an alternative mechanism for generating death signals. *Cell* **82**, 405–414
 36. Dbaiho, G. S., Pushkareva, M. Y., Rachid, R. A., Alter, N., Smyth, M. J., Obeid, L. M., and Hannun, Y. A. (1998) p53-dependent ceramide response to genotoxic stress. *J. Clin. Inv.* **102**, 329–339
 37. Cabot, M. C., Giuliano, A. E., Han, T. Y., and Liu, Y. Y. (1999) SDZ PSC 933, the cyclosporine A analogue and multidrug resistance modulator, activates ceramide synthase and increase vinblastine sensitivity in drug-sensitive and drug-resistant cancer cells. *Cancer Res.* **59**, 880–885
 38. Myrick, D., Blackinto, D., Klostergaard, J., Kouttab, N., Maizel, A., Wanebo, H., and Mehta, S. (1999) Paclitaxel-induced apoptosis in Jurkat, a leukemic T cell line, is enhanced by ceramide. *Leuk. Res.* **23**, 569–578
 39. Hannun, Y. A., and Luberto, C. (2000) Ceramide in the eukaryotic stress response. *Trends Cell Biol.* **10**, 73–80
 40. Luberto, C., and Hannun, Y. A. (1998) Sphingomyelin synthase, a potential regulator of intracellular levels of ceramide and diacylglycerol during SV40 transformation: does sphingomyelin synthase account for the putative phosphatidylcholine-specific phospholipase C? *J. Biol. Chem.* **273**, 14550–14559
 41. Marsh, N. L., Elias, P. M., and Holleran, W. M. (1995) Glucosylceramides stimulate murine epidermal hyperproliferation. *J. Clin. Invest.* **95**, 2903–2909
 42. Datta, S. C., and Radin, N. S. (1988) Stimulation of liver growth and DNA synthesis by glucosylceramide. *Lipids* **23**, 508–510
 43. Perales, M., Cervantes, F., Cobo, F., and Montserrat, E. (1998) Non-Hodgkin's lymphoma associated with Gaucher's disease. *Leuk. Lymphoma* **31**, 609–612
 44. Yokoyama, K., Suzuki, M., Kawashima, I., Karasawa, K., Nojima, S., Enomoto, T., Tai, T., Suzuki, A., and Setaka, M. (1997) Changes in composition of newly synthesized sphingolipids of HeLa cells during the cell cycle-suppression of sphingomyelin and higher-glycosphingolipid synthesis and accumulation of ceramide and glucosylceramide in mitotic cells. *Eur. J. Biochem.* **249**, 450–455
 45. Rani, C. S., Abe, A., Chang, Y., Rosenzweig, N., Saltiel, A. R., Radin, N. S., and Shayman, J. A. (1995) Cell cycle arrest induced by an inhibitor of glucosylceramide synthase: correlation with cyclin-dependent kinases. *J. Biol. Chem.* **270**, 2859–2867
 46. Kyogashima, M., Inoue, M., Seto, A., and Inokuchi, J. (1996) Glucosylceramide synthetase inhibitor, D-threo-1-phenyl-2-decanoilamino-3-morpholino-1-propanol exhibits a novel decarcinogenic activity against Shope carcinoma cells. *Cancer Lett.* **101**, 25–30
 47. Inokuchi, J., Jimbo, M., Momosaki, K., Shimeno, H., Nagamatsu, A., and Radin, N. S. (1990) Inhibition of experimental metastasis of murine Lewis lung carcinoma by an inhibitor of glucosylceramide synthase and its possible mechanism of action. *Cancer Res.* **50**, 6731–6737
 48. Fukumoto, H., Nishio, K., Ohta, S., Hanai, N., and Saijo, N. (1996) Reversal of adriamycin resistance with chimeric anti-ganglioside GM2 antibody. *Int. J. Cancer* **67**, 676–680
 49. Peterson, R. H., Meyers, M. B., Spengler, B. A., and Biedler, J. L. (1983) Alteration of plasma membrane glycopeptides and gangliosides of Chinese hamster cells accompanying development of resistance to daunorubicin and vincristine. *Cancer Res.* **43**, 222–228
 50. Birkle, S., Gao, L., Zeng, G., and Yu, R. K. (2000) Down-regulation of GD3 ganglioside and its O-acetylated derivative by stable transfection with antisense vector against GD3-synthase gene expression in hamster melanoma cells: effects on cellular growth, melanogenesis, and dendricity. *J. Neurochem.* **74**, 547–554
 51. Lucci, A., Han, T. Y., Liu, Y. Y., Giuliano, A. E., and Cabot, M. C. (1999) Multidrug resistance modulators and doxorubicin synergize to elevate ceramide levels and elicit apoptosis in drug-resistant cancer cells. *Cancer* **86**, 300–311

52. Lucci, A., Han, T. Y., Liu, Y. Y., Giuliano, A. E., and Cabot, M. C. (1999) Modification of ceramide metabolism increases cancer cell sensitivity to cytotoxics. *Int. J. Oncol.* **15**, 541–546
53. Radin, N. S. (1999) Chemotherapy by slowing glucosphingolipid synthesis. *Biochem. Pharmacol.* **57**, 589–595
54. Basu, S., Kaufman, B., and Roseman, S. (1968) Enzymatic synthesis of ceramide-glucose and ceramide-lactose by glycosyltransferase from embryonic chicken brain. *J. Biol. Chem.* **243**, 5802–5804
55. Kolter, T., and Sandhoff, K. (1998) Recent advances in the biochemistry of sphingolipidoses. *Brain Pathol.* **8**, 79–100
56. Simons, K., and Ikonen, E. (1997) Functional rafts in cell membranes. *Nature (London)* **387**, 569–572
57. Harder, T., and Simons, K. (1997) Caveolae, DIGs, and the dynamics of sphingolipid-cholesterol microdomains. *Curr. Opin. Cell Biol.* **9**, 534–542
58. Ferte, J. (2000) Analysis of the tangled relationships between P-glycoprotein-mediated multidrug resistance and the lipid phase of the cell membrane. *Eur. J. Biochem.* **267**, 277–294
59. Lavie, Y., Fiucci, G., Czarny, M., and Liscovitch, M. (1999) Changes in membrane microdomains and caveolae constituents in multidrug-resistant cancer cells. *Lipids* **34**, S57–S63
60. Iwabuchi, K., Yamamura, S., Prinetti, A., Handa, K., and Hakomori, S. (1998) GM3-enriched microdomain involved in cell adhesion and signal transduction through carbohydrate-carbohydrate interaction in mouse melanoma B16 cells. *J. Biol. Chem.* **273**, 9130–9138
61. Hakomori, S. (1998) Cancer-associated glycosphingolipid antigens: their structure, organization, and function. *Acta Anat.* **161**, 79–90
62. Yamashita, T., Wada, R., Sasaki, T., Deng, C., Bierfreund, U., Sandhoff, K., and Proia, R. L. (1999) A vital role for glycosphingolipid synthesis during development and differentiation. *Proc. Natl. Acad. Sci. USA* **96**, 9142–9147
63. Rosenwald, A. G., and Pagano, R. E. (1994) Effects of the glucosphingolipid synthesis inhibitor PDMP on lysosomes in cultured cells. *J. Lipid Res.* **35**, 1232–1240
64. Mizutani, A., Kuroda, Y., Muramoto, K., Kobayashi, K., Yamagishi, K., and Inokuchi, J. (1996) Effects of glucosylceramide synthase inhibitor and ganglioside GQ1b on synchronous oscillations of intracellular Ca²⁺ in cultured cortical neurons. *Biochem. Biophys. Res. Commun.* **222**, 494–498
65. Mutoh, T., Tokuda, A., Inokuchi, J. I., and Kuriyama, M. (1998) glucosylceramide synthase inhibitor inhibits the action of nerve growth factor in PC12 cells. *J. Biol. Chem.* **273**, 1998

Received for publication April 27, 2000.

Revised for publication August 7, 2000.